Top-quark mass and isospin breaking in the dynamical symmetry-breaking scenario

T. Asaka, Y. Shobuda, and Y. Sumino
Department of Physics, Tohoku University, Sendai, 980-77 Japan
(Received 1 May 1996)

We consider a scenario where the top-quark mass is generated dynamically, and study the implications of the present experimental values for m_t and the T parameter. We assume a technicolorlike scenario for inducing the W mass and an effective four-Fermi operator for inducing the top-quark mass. We also assume that only this four-Fermi operator is relevant at low energy. Then we estimate in detail the strength G and the intrinsic mass scale M of the four-Fermi operator. A unitarity bound is used to quantify the strength of G. We find that $G/4\pi \sim 1$ and that M is of the order of $\Lambda_{\rm TC} \simeq 1-2$ TeV or less. Namely the four-Fermi operator cannot be treated as ''pointlike'' around the electroweak scale. Furthermore we estimate the contribution of the four-Fermi operator to the T parameter. We find that the QCD correction to the top-quark mass function reduces the contribution to the T parameter by about 40%. By comparing the results with the present experimental bound, we obtain another upper bound on M which is typically in the several to 10 TeV region. [S0556-2821(96)02721-X]

PACS number(s): 14.65.Ha, 11.30.Qc

I. INTRODUCTION

The $SU(2)\times U(1)$ gauge theory for describing the electroweak interactions has been very successful both theoretically and experimentally. However, all experimental tests have been done for its gauge part and we have little knowledge on the electroweak symmetry-breaking mechanism so far. In light of the naturalness problem, we may suppose that there exists some new physics related to electroweak symmetry breaking at the energy scale 100 GeV–1 TeV. Dynamical symmetry breaking is one of the attractive candidates for a solution to the naturalness problem. We consider this possibility and study the implications of the present experimental data for the top-quark mass [1] and the T parameter [2–4].

In dynamical symmetry-breaking scenarios such as technicolor models, an effective four-Fermi operator

$$\mathcal{L} = \frac{1}{\Lambda^2}\overline{U_L}U_R\overline{t_R}t_L + \text{H.c.} \tag{1}$$

is introduced in order to generate the top-quark mass, where Λ represents the new physics scale (extended technicolor scale) and U denotes a new fermion (technifermion) introduced in the symmetry-breaking sector. When this fermion forms a pair condensate $\langle \overline{U_L}U_R \rangle \neq 0$, the top quark acquires its mass

$$m_t \sim \frac{\langle \overline{U_L}U_R \rangle}{\Lambda^2}. \tag{2}$$

Because the condensate also gives mass to the W boson, one may naively expect that the condensate has the same order of magnitude as the electroweak symmetry-breaking scale:

$$\langle \overline{U_L}U_R \rangle^{1/3} \sim \Lambda_{\rm EW} \sim 1 \text{ TeV}. \tag{3}$$

From the observed value of the top-quark mass $m_t \simeq 175$ GeV [1], this naive argument suggests that $1/\Lambda^2 \sim m_t/\Lambda_{\rm EW}^3$ and that the new physics scale Λ is not too far from $\Lambda_{\rm EW}$.

During the last decade, there were many analyses of the dynamical symmetry-breaking scenarios in the case of a large top-quark mass $m_t > 100$ GeV. In 1985, Appelquist *et al.* [5] studied the ρ parameter (T parameter) in the context of extended technicolor models. They pointed out that naively the mass difference between the techni-U and its isopartner techni-D is proportional to the top-quark mass, so that this difference would contribute to the T parameter. Also, they noted that an extra isospin-violating operator

$$\frac{1}{\Lambda'^2}\overline{Q_R}\gamma^\mu\sigma^3 Q_R \overline{Q_R}\gamma_\mu\sigma^3 Q_R, \tag{4}$$

where $Q_R = (U_R, D_R)^T$, may give a large contribution to the T parameter since Λ' is considered to approximate Λ. (For $m_t \simeq 175$ GeV, the latter effect would be more significant than the former.) It was suggested in Ref. [6] that the T parameter would be enhanced in the walking technicolor scenario. More detailed analyses on the T parameter were given later in Refs. [7,8]. Recently the experimental constraint on the T parameter has become more severe, and deviation from the standard model prediction is seen to be very small [4]. Reflecting the present constraint, some dynamical symmetry-breaking models have been proposed [9,10] in which the operator (4) is suppressed at low energy. Reference [11] studied the constraints from the present T parameter and top-quark mass data, and discussed the top-color-assisted technicolor model in this context.

In this paper we assume that at low energy the four-Fermi operators other than Eq. (1) can be neglected. We estimate the strength and the intrinsic mass scale of the particular operator (1) in detail based on this assumption. Since it is a (nonrenormalizable) effective operator, the tree-level unitarity of some processes induced by this operator is violated above some energy. This fact is used to quantify the intrinsic

 © 1996 The American Physical Society

mass scale of the operator. Then we estimate the contribution of this operator to the T parameter. We include the QCD correction to the top-quark mass function and study its effect on the T parameter.

In order to incorporate the dynamics of symmetry breaking into our analyses, we solve numerically the Schwinger-Dyson and Bethe-Salpeter equations in the improved-ladder approximation [12]. We follow the formalism developed in Refs. [13–15]; in these papers, taking $f_\pi = 94$ MeV as the only input parameter for QCD, the quantities $\Lambda_{\rm QCD}$, $\langle \bar{\Psi}\Psi \rangle$, m_ρ, m_{a_1}, m_{a_0}, f_ρ, and f_{a_1} have been calculated, which meet the experimental values within 20–30 % accuracy for $\Lambda_{\rm QCD}, \ldots, m_{a_0}$ and within a factor of 2 for f_ρ and f_{a_1}. Thus, we expect to study the dynamical effect semiquantitatively using the formalism.

In Sec. II we present our assumption on the dynamical symmetry-breaking scenario. Then we estimate the strength of the four-Fermi operator from the observed top-quark mass and W boson mass in Sec. III. Using the result, the contributions to the T parameter are estimated in Sec. IV. The conclusion and discussion are given in Sec. V.

The explicit formulas of the Schwinger-Dyson and Bethe-Salpeter equations, as well as other equations used in our numerical analyses, are collected in the Appendix.

II. SYMMETRY-BREAKING SECTOR AND FOUR-FERMI OPERATOR

In this section we explain our assumption on the scenario of the dynamical generation of the top-quark mass.

First, we assume a technicolorlike scenario [16] for breaking electroweak gauge symmetry. We introduce nonstandard-model fermions following the one-doublet technicolor (TC) model as

$$Q_L = \begin{pmatrix} U \\ D \end{pmatrix}_L, \quad U_R, \ D_R. \tag{5}$$

The weak hypercharges are assigned as $Y(Q_L) = 0$, $Y(U_R) = 1/2$, and $Y(D_R) = -1/2$. These fermions belong to the fundamental representation of the SU($N_{\rm TC}$) gauge group, and they form the pair condensates

$$\langle \overline{U_L} U_R \rangle \neq 0 \quad \text{and} \quad \langle \overline{D_L} D_R \rangle \neq 0 \tag{6}$$

via the SU($N_{\rm TC}$) gauge interaction. Later, when we solve the Schwinger-Dyson equations numerically, we will deal with both the technicolorlike and walking-technicolor-like [17] scenarios by varying the running behavior of the gauge coupling constant. In the following analyses, we consider only the cases $N_{\rm TC} = 2$ and 3, taking into account the present stringent experimental constraint [4] on the S parameter [2].

Second, in order to generate the top-quark mass, we introduce an effective four-Fermi operator

$$\frac{G}{M^2} (\overline{Q_L} U_R)(\overline{t_R} q_L) + \text{H.c.}, \tag{7}$$

where q_L denotes the ordinary quark doublet $(t_L, b_L)^T$. G is a dimensionless coupling and M is the intrinsic mass scale of this operator. Because the four-Fermi operator cannot be a fundamental interaction, there should be some energy scale above which this operator will resolve, and we call this scale M. In other words, it is the scale where higher dimensional operators neglected in Eq. (7) become relevant. We may neglect the higher dimensional operators if all the energy scales involved in our calculation satisfy $E/M \ll 1$. In particular, since we will incorporate the nonperturbative dynamics of the SU($N_{\rm TC}$) technicolor interaction by solving the Schwinger-Dyson and Bethe-Salpeter equations, the validity of our effective treatment of the four-Fermi operator (7) as a contact interaction would be justified if the technicolor scale $\Lambda_{\rm TC}$ satisfies $\Lambda_{\rm TC} \ll M$.

We assume that we may neglect all effective four-Fermi operators other than Eq. (7) which would be induced at low energy in the models such as extended technicolor models [18]. (See, however, the discussion in Sec. V.) This is because an operator such as Eq. (4) would give a very large contribution to the T parameter. We do not consider the dynamical origin of the operator (7) in this paper.

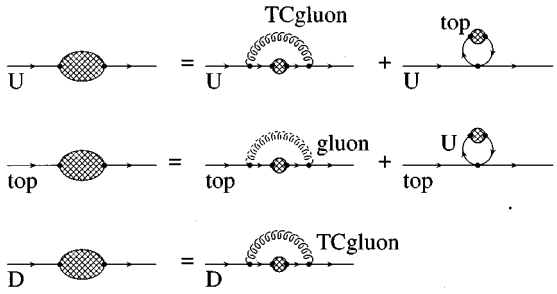

FIG. 1. The graphical representation for the coupled Schwinger-Dyson equations for the mass functions of techni-U and top quark, and for the Schwinger-Dyson equation for the mass function of techni-D.

III. STRENGTH AND MASS SCALE OF THE FOUR-FERMI OPERATOR

In this section, we estimate the strength G and the intrinsic mass scale M of the four-Fermi operator (7) from the observed top-quark and W-boson masses.

A. Relation between G and M

We solve numerically the coupled Schwinger-Dyson equations for the techni-U and top quark as well as the Schwinger-Dyson equation for techni-D. (See the Appendix for details.) These equations are depicted diagrammatically in Fig. 1. In order to set a mass scale in the numerical calculation, we use the charged decay constant $F_{\pi^\pm}$, which is calculated using the generalized Pagels-Stokar formula [21]. From the W-boson mass M_W, $F_{\pi^\pm}$ is normalized as

$$F_{\pi^\pm} = \frac{2M_W}{g} \simeq 250 \ \text{GeV}, \tag{8}$$

where g is the SU(2)$_L$ gauge coupling constant. Also, we input the top-quark mass to be $\Sigma_t(m_t^2) = m_t \simeq 175$ GeV [1]. These two inputs relate the coupling G and the intrinsic mass scale M of the four-Fermi operator (7).

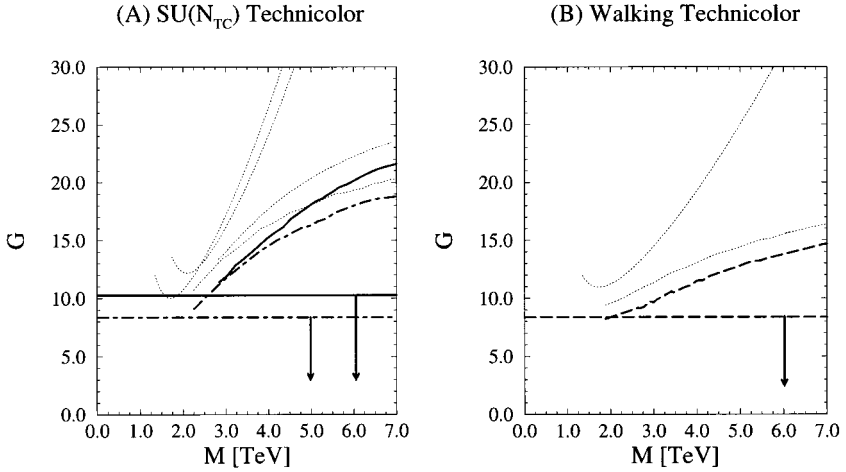

FIG. 2. The allowed regions in the G-M plane obtained by solving the coupled Schwinger-Dyson equations for (A) SU($N_{\rm TC}$) technicolor cases and for (B) the walking-technicolor case. Curved lines represent the coupling $G(M)$. Horizontal lines show the upper bounds for G obtained from the unitarity limit. For SU($N_{\rm TC}$) technicolor cases, the solid and dot-dashed lines correspond to $N_{\rm TC}=2$ and $N_{\rm TC}=3$, respectively. For comparison, also shown as dots is the coupling $G(M)$ when the QCD correction to the top-quark mass function and the top-loop contribution to the techni-U mass function are switched off successively.

Let us demonstrate the relation between G and M in the simple case where we can neglect both the top-loop contribution of the Schwinger-Dyson equation for the techni-U and the QCD correction of the equation for the top quark. In this case the top-quark mass can be calculated from the mass function of the techni-U, Σ_U, as

$$m_t=\frac{G}{M^2}\langle\overline{U_L}U_R\rangle_M, \tag{9}$$

where

$$\langle\overline{U_L}U_R\rangle_M=\frac{1}{2}\int_{p_E^2\le M^2}\frac{d^4p}{(2\pi)^4}\mathrm{tr}\left(\frac{i}{\not p-\Sigma_U(p)}\right)$$
$$=\frac{N_{\rm TC}}{8\pi^2}\int_0^{M^2}dx\frac{x\Sigma_U(x)}{x+\Sigma_U(x)^2}, \tag{10}$$

with $x=p_E^2=-p^2$. Note that we define the intrinsic mass scale M of the four-Fermi operator (7) as the momentum cutoff of the integral in Eq. (10) since the four-Fermi operator will resolve above the energy scale M. By calculating the condensate $\langle\overline{U_L}U_R\rangle_M$ for a given M, and substituting the top-quark mass $m_t\simeq 175$ GeV in Eq. (9), we obtain the coupling G as a function of M.

Now returning to the solution to the coupled Schwinger-Dyson equations (Fig. 1), we show the G-M relation in Fig. 2 for the SU(2) and SU(3) technicolor cases, and also for the walking-technicolor case.[1] We neglect the region $M\lesssim\Lambda_{\rm TC}$ where our effective treatment of the four-Fermi operator (7) as a contact interaction breaks down. We define $\Lambda_{\rm TC}$ as the scale where the leading-logarithmic running coupling constant of technicolor diverges. The values of $\Lambda_{\rm TC}$ in our numerical estimates are $\Lambda_{\rm TC}\simeq 1.7$, 1.3, and 0.6 TeV for the SU(2), SU(3) technicolor, and the walking-technicolor cases, respectively. We see that $G(M)$ increases with M for each case. It should be noted that for both technicolor and walking-technicolor cases, the coupling G should be rather strong, typically $G/4\pi\sim O(1)$ in order to explain the observed top-quark mass.

We also show as dotted lines in these figures the G-M relation in the case without a QCD correction to the top-quark mass function. We find that the QCD effect decreases the coupling $G(M)$. This is because for $\mu>m_t$ the top-quark mass becomes smaller, $\Sigma_t(\mu^2)<m_t$, due to the QCD correction

$$\Sigma_t(\mu^2)=\Sigma_t(m_t^2)\left[\frac{\ln(m_t^2/\Lambda_{\rm QCD}^2)}{\ln(\mu^2/\Lambda_{\rm QCD}^2)}\right]^{4/\beta}, \tag{11}$$

where $\beta=11-2n_f/3$ is the lowest order coefficient of the β function of the QCD renormalization group equation, so that a weaker coupling G is necessary to generate the top-quark mass.

We further switch off the second term on the right-hand side of the Schwinger-Dyson equation for the techni-U, namely, the contribution of the top-quark loop via the operator (7). The neglect of the top-quark contribution would have been justified if the coupling G were small and the intrinsic mass scale M were large, $M\gg\Lambda_{\rm TC}$. Note that the operator (7) affects the mass function of techni-U but not that of techni-D. The change in the G-M relation in this case is also shown as dots in the same figures. The effect of the top-quark contribution can be understood as follows. The top-quark loop diagram in Fig. 1 gives additive contribution to $\langle\overline{U_L}U_R\rangle_M$ so that the coupling G is reduced. The effect increase for larger M since the coupling G is larger in this region.

B. Unitarity constraint for the coupling G

We have seen that the coupling G should be quite large. As a criterion for testing the strength of G, we study the tree-level unitarity limit related to the four-Fermi operator (7). There are a few scattering amplitudes induced by this operator at the tree level which increase in high energy and at some energy would violate the unitarity bound. The tree-level unitarity violation occurs at lower energy for a larger value of G in general. However, the energy to reach the

[1]In our analyses, the walking-technicolor case corresponds to the SU(3) technicolor theory with one technifermion doublet which is introduced in Eq. (5) and ten technifermion singlets under $\mathrm{SU}(2)_L\times\mathrm{U}(1)_Y$. The one-loop β function reduces to approximately 1/3 of the SU(3) technicolor case.

unitarity limit should be above the scale M, since we have assumed that the four-Fermi operator (7) can be treated as a contact interaction below the scale M; that is, the higher dimensional operators are irrelevant at energy scale $E \ll M$. We see that this requirement leads to the upper bound for G.

Let us consider the two-body to two-body scatterings of fermions via the operator (7) at the energy scale where $E \gg \Lambda_{\rm TC}$. In this energy region the confinement effect of technicolor may be ignored. The tree-level matrix elements of these processes increase quadratically with the center-of-mass energy. We find that the scattering amplitude for $tt \to UU$ in the $J=0$ channel will reach the unitarity limit most quickly. The partial-wave amplitude is given by

$$T^{J=0}(\sqrt{s}) = \frac{\sqrt{N_C N_{\rm TC}}}{8\pi} \frac{G}{M^2} s, \tag{12}$$

where $\sqrt{s}$ is the center-of-mass energy.[2] We set $m_t = m_U = 0$ considering $E \gg \Lambda_{\rm TC}$. Unitarity limit [20] for an inelastic scattering channel is given by $|T^J| \leqslant 1$. We may demand that the tree-level unitarity should not be violated below $\sqrt{s} = M$, that is,

$$|T^{J=0}(\sqrt{s}=M)| \leqslant 1, \tag{13}$$

which can be translated to the upper bound for G as

$$G \leqslant \frac{8\pi}{\sqrt{N_C N_{\rm TC}}}. \tag{14}$$

The bound is so stringent that there are hardly allowed regions in the G-M planes in Fig. 2 for $M > \Lambda_{\rm TC}$. This result suggests that our effective treatment of the four-Fermi operator as a contact interaction breaks down. Since the coupling G exceeds the perturbative unitarity limit for $M > \Lambda_{\rm TC}$, the higher order corrections of G are large and should modify the tree-level amplitude to restore unitrairy at energy scale $E \sim \Lambda_{\rm TC}$. Such corrections induce the higher dimensional operators which become relevant at an energy scale $E \sim \Lambda_{\rm TC}$. Thus the scale M above which the operator (7) will resolve is found to be around $\Lambda_{\rm TC}$ or less.

IV. CONTRIBUTIONS TO THE T PARAMETER

Because the four-Fermi operator (7) violates isospin symmetry, one may expect that the results obtained in the previous section may lead to large isospin-violating effects. In this section we estimate the contributions of the four-Fermi operator to the T parameter.

A. Contribution of $\Sigma_U - \Sigma_D$

Here we consider the isospin-violating effect originating from the difference of techni-U and techni-D mass functions. The contribution of the four-Fermi operator to the techni-U mass function in the Schwinger-Dyson equations causes this difference. (See Fig. 1.) We estimate the T parameter and compare with the present experimental bound, from which we extract another bound for the mass scale M of the four-Fermi operator.

We calculate the charged and neutral decay constants $F_{\pi^\pm}$ and F_{π^0} from the mass functions of techni-U and D using the generalized Pagels-Stokar formula [21]. Then the contribution to the T parameter ($T_{\rm new}$) is calculated as

$$\alpha T_{\rm new} = \frac{F_{\pi^\pm}^2 - F_{\pi^0}^2}{F_{\pi^0}^2}, \tag{15}$$

where $\alpha = 1/128$ is the fine structure constant. Thus, we can calculate $T_{\rm new}$ as a function of G and M.

Let us first neglect the QCD effect on Σ_t. The results are shown in Fig. 3 when the coupling G is on the corresponding dotted lines $G = G(M)$ in Fig. 2. One sees that $T_{\rm new}$ increases with M (or G). This behavior is consistent with the naive estimate of T parameter by the fermion one-loop calculation [2]

$$T \simeq \frac{N_{\rm TC}}{12\pi \sin^2\theta_W \cos^2\theta_W} \left[\frac{(\Delta m)^2}{M_Z^2} \right], \tag{16}$$

combined with a naive estimate of the mass difference of techni-U and D from the coupled Schwinger-Dyson equations (i.e., the top-loop contribution in Fig. 1)

$$\Delta m \simeq \frac{N_C}{8\pi^2} G(M) m_t. \tag{17}$$

Also we see that $T_{\rm new}$ is larger for the walking-technicolor case than that of technicolor case for the same M. This tendency has been pointed out by Chivukula [6].

Comparing the results with the present experimental data on the T parameter [4]

$$T_{\rm expt} - T_{\rm SM}(m_t = 175\ {\rm GeV}, m_H = 1\ {\rm TeV}) = 0.32 \pm 0.20, \tag{18}$$

we may put 3σ upper bounds for the intrinsic mass scale M as follows:

$$\begin{aligned} M &\lesssim 7\ {\rm TeV} \quad \text{for SU(2) technicolor}, \\ M &\lesssim 5\ {\rm TeV} \quad \text{for SU(3) technicolor}, \\ M &\lesssim 4\ {\rm TeV} \quad \text{for walking technicolor}. \end{aligned} \tag{19}$$

Note that the bound is more stringent for the walking-technicolor case.

Next, we inculde the QCD correction on Σ_t. The results are also shown in Fig. 3. Note that the QCD correction reduces $T_{\rm new}$ by about 40%. This can be understood from Eqs. (16) and (17) if we note that both $G(M)$ and $\Sigma_t(\mu^2)$ ($\mu > m_t$) get smaller by the QCD correction. (See Sec. III A). Similarly, 3σ upper bounds for M are obtained:

[2] In our previous paper [19], we incorrectly omitted the color and technicolor factors in Eq. (12) which come from the normalization of the initial and final states.

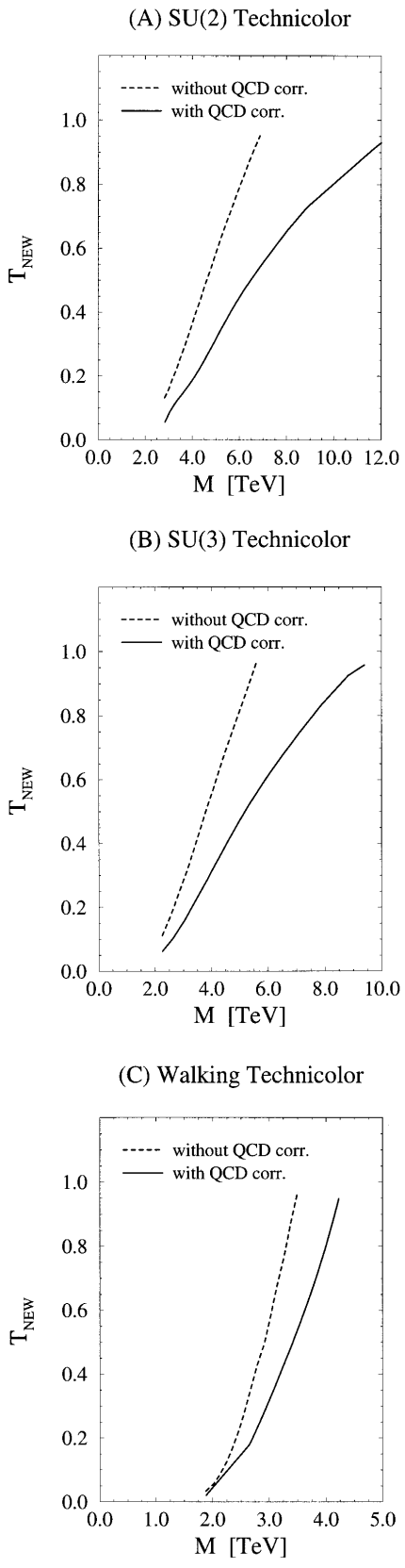

FIG. 3. The contribution to the T parameter, $T_{\rm new}$, from $\Sigma_U-\Sigma_D$ when the coupling is on the curved lines $G=G(M)$ in Fig. 2, for (A) SU(2) technicolor, (B) SU(3) technicolor, and (C) walking-technicolor cases. The dotted lines are $T_{\rm new}$ without a QCD correction and the solid lines are the ones including the QCD correction.

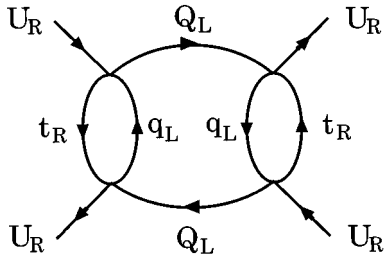

FIG. 4. A three-loop Feynman diagram that induces the operator $\overline{U_R}\gamma^\mu U_R\overline{U_R}\gamma_\mu U_R$.

$$M\lesssim 12\ \text{TeV}\quad \text{for SU(2) technicolor},$$

$$M\lesssim 9\ \text{TeV}\quad \text{for SU(3) technicolor},$$

$$M\lesssim 4\ \text{TeV}\quad \text{for walking technicolor}. \tag{20}$$

B. Contribution of $\overline{U_R}\gamma_\mu U_R\overline{U_R}\gamma^\mu U_R$

We started our analyses assuming that only the four-Fermi operator (7) exists at low energy in order to dispense with the potentially dangerous operator

$$C\overline{U_R}\gamma_\mu U_R\overline{U_R}\gamma^\mu U_R, \tag{21}$$

which would induce a large T parameter [5]. We found in the previous section, however, that the higher order corrections of the operator (7) cannot be neglected. In fact, the above operator (21) is generated by four insertions of the operator (7) at three-loop level (Fig. 4). From a dimensional analysis of this graph, we estimate

$$C\sim -\frac{N_C^2}{(4\pi)^6}\frac{G^4}{M^2}. \tag{22}$$

Then the contribution of the operator (21) to the T parameter can be estimated as

$$T\sim 6\times 10^{-2}\frac{N_{\rm TC}(N_{\rm TC}+1)}{12}\left(\frac{m_U}{1\,\text{TeV}}\right)^4\left(\frac{2\,\text{TeV}}{M}\right)^2 \times\left(\frac{G}{4\pi}\right)^4\left(\ln\frac{\Lambda_{\rm TC}^2}{m_U^2}\right)^2. \tag{23}$$

We should note that the three-loop graph is very sensitive to the cutoff of the loop momenta. Therefore the estimated value, Eq. (23), may change by a factor ~ 10 by a slight change of the cutoff and therefore it may give a non-negligible contribution to the T parameter. We should also remark that Eq. (22) may suggest self-inconsistency of our assumption that we neglect all four-Fermi operators other than Eq. (7). We will discuss this point in the next section.

V. CONCLUSION AND DISCUSSION

In this paper, within a scenario where the top-quark mass is generated dynamically, we estimated the coupling G and the intrinsic mass scale M of the four-Fermi operator that induces the top-quark mass. Also, we studied the contribu-

tion of this four-Fermi operator to the T parameter.

Throughout our analyses, we made the following assumptions.

The W and Z bosons acquire their masses in the one-doublet technicolorlike scenario.

The top quark acquires its mass via the effective four-Fermi operator (7). We consider only this four-Fermi operator and neglect all other effective four-Fermi operators that may be induced in various dynamical models.

We incorporated the dynamics of a SU($N_{\rm TC}$) gauge interaction by solving the Schwinger-Dyson and Bethe-Salpeter equations numerically in the improved-ladder approximation (in all the analyses except in Sec. IV B).

In Sec. III, we studied in detail the strength G and the intrinsic mass scale M of the four-Fermi operator using M_W and m_t as the input parameters. We obtained G as a function of M in the region $M>\Lambda_{\rm TC}$, and found that G is rather strong, $G/4\pi\sim O(1)$. Then we compared the coupling G with that demanded by the tree-level unitarity bound. Our results suggest that M should be of the order of $\Lambda_{\rm TC}\simeq 1\sim 2$ TeV or less, so that the four-Fermi operator cannot be treated as ''pointlike'' at scale $E\sim\Lambda_{\rm TC}$. Conventionally the four-Fermi operator (7) has been treated perturbatively in many papers, but the unitarity saturation shows that such a treatment is inconsistent with the presently observed top-quark mass. We included part of the higher order corrections of the four-Fermi operator (7) by solving the coupled Schwinger-Dyson equations. Also we included the effect of a QCD correction on the top-quark mass function. These effects, respectively, are found to reduce $G(M)$.

In Sec. IV we studied the contributions of the four-Fermi operator (7) to the T parameter. First we estimated the contribution of the difference between the mass functions of techni-U and techni-D. We found that the QCD correction is large and reduces the contribution to the T parameter by about 40%. The estimated T parameter is within the present experimental bound. Then we used the experimental bound to obtain another upper bound for M, and found that typically M is less than 10 TeV. The bound on M is more stringent for the walking-technicolor case. Second, we pointed out that the dangerous operator $\overline{U_R}\gamma_\mu U_R\overline{U_R}\gamma^\mu U_R$ would be generated by the four-Fermi operator (7) at the three-loop level, and estimated its contribution to the T parameter from a dimensional analysis. The contribution may become non-negligible.

We found that the four-Fermi operator (7) cannot be treated as ''pointlike'' at the scale $E\sim\Lambda_{\rm TC}$. In order to make a more consistent analysis, one needs to specify the ''structure'' of the four-Fermi operator, i.e., specify the dynamical origin of this operator. One way is to rewrite the four-Fermi operator in terms of a massive-gauge-boson exchange interaction as in extended technicolor models. We are currently making further analyses in this direction.

We started our analyses on the assumption that all four-Fermi operators except Eq. (7) can be neglected. We found, however, that other four-Fermi operators generated in higher orders of the operator (7) may be non-negligible (e.g., the operator $\overline{U_R}\gamma_\mu U_R\overline{U_R}\gamma^\mu U_R$). This self-inconsistency seems to impose certain constraints when constructing a viable model of dynamical electroweak symmetry breaking. Namely, suppose one could construct an extended technicolor model that has ETC gauge bosons which induce only the four-Fermi operator (7) at the tree level. Then other four-Fermi operators induced at higher loops would be suppressed by powers of $\Lambda_{\rm TC}/M$, but this factor is close to 1 for the top-quark mass $\simeq 175$ GeV.

ACKNOWLEDGMENTS

We are grateful to K. Fujii, K. Hagiwara, K. Hikasa, J. Hisano, B. Holdom, N. Maekawa, T. Moroi, H. Murayama, M. Peskin, and J. Terning for fruitful discussion.

APPENDIX

In this appendix, we list the Schwinger-Dyson equations as well as other formulas which are used in our numerical analyses.

In Sec. III, we solved the coupled and noncoupled Schwinger-Dyson equations in the improved-ladder approximation for the mass functions of techni-U, techni-D, and top quark (Σ_U, Σ_D, and Σ_t). All these equations can be written in the forms:[3]

$$\Sigma_U(x)=\frac{\lambda(x)}{4x}\int_0^x dy\frac{y\Sigma_U(y)}{y+\Sigma_U^2(y)}+\int_x^{M^2}dy\frac{\lambda(y)\Sigma_U(y)}{4[y+\Sigma_U^2(y)]}+\frac{N_C}{8\pi^2}\frac{G}{M^2}\int_0^{M^2}dy\frac{y\Sigma_t(y)}{y+\Sigma_t^2(y)},$$

$$\Sigma_D(x)=\frac{\lambda(x)}{4x}\int_0^x dy\frac{y\Sigma_D(y)}{y+\Sigma_D^2(y)}+\int_x^{M^2}dy\frac{\lambda(y)\Sigma_D(y)}{4[y+\Sigma_D^2(y)]},$$

$$\Sigma_t(x)=\frac{N_{\rm TC}}{8\pi^2}\frac{G}{M^2}\int_0^{M^2}dy\frac{y\Sigma_U(y)}{y+\Sigma_U^2(y)}+\frac{\lambda_{\rm QCD}(x)}{4x}\int_0^x dy\frac{y\Sigma_t(y)}{y+\Sigma_t^2(y)}+\int_x^{M^2}dy\frac{\lambda_{\rm QCD}(y)\Sigma_t(y)}{4[y+\Sigma_t^2(y)]},\tag{A1}$$

where $\lambda(x)$ and $\lambda_{\rm QCD}(x)$ denote the running coupling constants for technicolor and color interactions, respectively.

According to Ref. [13], we take $\lambda(x)$ as:

$$\lambda(x)=\lambda_0\times\begin{cases}C & \text{if } t\leq t_0,\\ C-\frac{1}{2}\frac{A}{(1+At_{IF})^2}\frac{(t-t_0)^2}{(t_{IF}-t_0)} & \text{if } t_0\leq t\leq t_{IF},\\ \frac{1}{1+At} & \text{if } t_{IF}\leq t,\end{cases}\tag{A2}$$

[3]Here, note that the four-Fermi operator (7) resolves (and is crudely set equal to zero) above the scale M. For the technigluon's and gluon's loop diagrams, we replace the ultraviolet cutoff scale by M approximately, because the mass functions and the running coupling constants decrease in the energy region $x\gg\Lambda_{\rm TC}$.

with

$$t=\ln x \quad \text{and} \quad C=\frac{1}{2}\frac{A(t_{IF}-t_0)}{(1+At_{IF})^2}+\frac{1}{1+At_{IF}},$$

where $\lambda_0/A=12C_2/\beta_0$ and β_0 is the one loop order coefficient of the β function and $C_2=(N_{\rm TC}^2-1)/2N_{\rm TC}$ represents the second Casimir. Thus, above the infrared cutoff scale $t\geqslant t_{IF}$, $\lambda(x)$ is related to the one-loop running coupling constant $g_{\rm TC}(x)$ as

$$\lambda(x)=\frac{3}{4\pi^2}C_2 g_{\rm TC}^2(x). \tag{A3}$$

In our numerical calculation, we fix the point $t_0=\ln\mu_0^2$ relative to $\Lambda_{\rm TC}$ and consider the infrared cutoff scale t_{IF} as a free parameter. We define $\Lambda_{\rm TC}$ as the point where the leading logarthmic running coupling constant diverges:

$$1+A\ln\Lambda_{\rm TC}^2=0. \tag{A4}$$

As for all the dimensionful quantities in our calculation, we set the scale by normalizing the decay constant as in Eq. (8).

For the QCD coupling constant, $\lambda_{QCD}(x)$ takes the same form as Eq. (A2). Above the infrared cutoff scale of QCD, $\lambda_{\rm QCD}(x)$ can be expressed by the one-loop running coupling constant $g_{\rm QCD}(x)$ as

$$\lambda_{\rm QCD}(x)=\frac{3}{4\pi^2}C_2^{\rm QCD} g_{\rm QCD}^2(x). \tag{A5}$$

where $C_2^{\rm QCD}=(N_C^2-1)/2N_C$ and $N_C=3$. We set the mass scale of QCD by taking $\Lambda_{\rm QCD}=200$ MeV.

As mentioned earlier, we calculated the charged decay constant $F_{\pi^\pm}$ in order to set the mass scale. We define the decay constant as

$$\langle 0|\overline{Q_L}\gamma^\mu T^b Q_L(0)|\pi^a(q)\rangle=\frac{i}{2}F_\pi^{ab}q^\mu, \tag{A6}$$

where T^a $(a=1,2,3)$ is the generator of $SU(2)_L$. Then the charged and neutral decay constants, respectively, are given by $F_{\pi^\pm}\equiv F_\pi^{11}=F_\pi^{22}$ and $F_{\pi^0}\equiv F_\pi^{33}$

We calculate the charged decay constant $F_{\pi^\pm}$ and the neutral one F_{π^0} using the generalized Pagels-Stokar formulas [21]

$$F_{\pi^0}^2=\frac{N_{\rm TC}}{8\pi^2}\int_0^\infty dx I_0(\Sigma_U,\Sigma_D), \tag{A7}$$

$$F_{\pi^\pm}^2=\frac{N_{\rm TC}}{8\pi^2}\int_0^\infty dx I_\pm(\Sigma_U,\Sigma_D), \tag{A8}$$

with

$$I_0(\Sigma_U,\Sigma_D)\equiv x\frac{\Sigma_U^2-\frac{x}{4}\frac{d}{dx}\Sigma_U^2}{(x+\Sigma_U^2)^2}+x\frac{\Sigma_D^2-\frac{x}{4}\frac{d}{dx}\Sigma_D^2}{(x+\Sigma_D^2)^2}, \tag{A9}$$

$$I_\pm(\Sigma_U,\Sigma_D)\equiv x\frac{\Sigma_U^2+\Sigma_D^2-\frac{x}{4}\frac{d}{dx}(\Sigma_U^2+\Sigma_D^2)}{(x+\Sigma_U^2)(x+\Sigma_D^2)} + \frac{x^2}{2}\frac{\Sigma_U^2-\Sigma_D^2}{(x+\Sigma_U^2)(x+\Sigma_D^2)}\frac{d}{dx}\ln\left[\frac{x+\Sigma_U^2}{x+\Sigma_D^2}\right]. \tag{A10}$$

In our calculation, we cut off the integral at M instead of infinity in Eqs. (A7) and (A8). The approximation would be valid since $\Sigma_U(x)$ and $\Sigma_D(x)$ vanish swiftly the region $x\gg\Lambda_{\rm TC}^2$.

[1] CDF Collaboration, F. Abe *et al.*, Phys. Rev. Lett. **74**, 2626 (1995); D0 Collaboration, S. Abachi *et al.*, *ibid.* **74**, 2632 (1995).

[2] M. Peskin and T. Takeuchi, Phys. Rev. Lett. **65**, 964 (1990); Phys. Rev. D **46**, 381 (1992).

[3] C. Burgess, S. Godfrey, H. König, D. London, and I. Maksymyk, Phys. Rev. D **49**, 6115 (1994); K. Hagiwara, D. Haidt, C. S. Kim, and S. Matsumoto, Z. Phys. C **64**, 559 (1994).

[4] S. Matsumoto, Mod. Phys. Lett. A **10**, 2553 (1995).

[5] T. Appelquist, M. J. Bowick, E. Cohler, and A. I. Hauser, Phys. Rev. Lett. **53**, 1523 (1984); Phys. Rev. D **31**, 1676 (1985).

[6] R. Chivukula, Phys. Rev. Lett. **61**, 2657 (1988).

[7] T. Appelquist, T. Takeuchi, M. B. Einhorn, and L. C. R. Wijewardhana, Phys. Lett. B **232**, 211 (1989).

[8] M. B. Einhorn and D. Nash, Nucl. Phys. **B371**, 32 (1992) .

[9] B. Holdom, Phys. Lett. B **336**, 85 (1994).

[10] T. Asaka (in preparation).

[11] R. Chivukula, B. Dobrescu, and J. Terning, Report No. hep-ph/9506450 (unpublished).

[12] V. A. Miransky, Sov. J. Nucl. Phys. **38**, 280 (1984); K. Higashijima, Phys. Rev. D **29**, 1228 (1984).

[13] K. -I. Aoki, M. Bando, K. Hasebe, T. Kugo, and H. Nakatani, Prog. Theor. Phys. **82**, 1151 (1989); K.-I. Aoki, M. Bando, T. Kugo, M. G. Mitchard, and H. Nakatani, *ibid.* **84**, 683 (1990).

[14] K. -I. Aoki, T. Kugo, and M. G. Mitchard, Phys. Lett. B **266**, 467 (1991).

[15] M. Bando, M. Harada, and T. Kugo, Prog. Theor. Phys. **13**, 947 (1976); **91**, 927 (1994).

[16] S. Weinberg, Phys. Rev. D **13**, 947 (1976); **19**, 1277 (1979); L. Susskind, *ibid.* **20**, 2619 (1979); For review, see E. Farhi and L. Susskind, Phys. Rep. **74**, 277 (1981).

[17] B. Holdom, Phys. Lett. **150B**, 301 (1985); K. Yamawaki, M. Bando, and K. Matumoto, Phys. Rev. Lett. **56**, 1335 (1986); T. Akiba and T. Yanagida, Phys. Lett. **169B**, 432 (1986); T. Appelquist, D. Karabali, and L.C.R. Wijewardhana, Phys. Rev. Lett. **57**, 957 (1986).

[18] S. Dimopoulos and L. Susskind, Nucl. Phys. **B155**, 237 (1979); E. Eichten and K. Lane, Phys. Lett. **90B**, 125 (1980).

[19] T. Asaka, N. Maekawa, T. Moroi, Y. Shobuda, and Y. Sumino, in Proceedings of the Fifth Workshop on Japan Linear Collider, Kawatabi, Japan, 1995, edited by T. Kurihara, KEK Proceedings 95-11, 1995

[20] C. Itzykson and J. Zuber, *Quantum Field Theory* (McGraw-Hill, New York, 1980).

[21] V. A. Miransky, M. Tanabashi, and K. Yamawaki, Phys. Lett. B **221**, 177 (1989); Mod. Phys. Lett. A **4**, 1043 (1989).